



LAWRENCE
LIVERMORE
NATIONAL
LABORATORY

LLNL-TR-847638

Neutron inelastic scattering measurements on KCl and NaCl samples at the Dome

M. A. Stoyer, B. Longfellow, M. Burks, P. L. Kerr,
V. V. Mozin, E. Rubino

April 14, 2023

Disclaimer

This document was prepared as an account of work sponsored by an agency of the United States government. Neither the United States government nor Lawrence Livermore National Security, LLC, nor any of their employees makes any warranty, expressed or implied, or assumes any legal liability or responsibility for the accuracy, completeness, or usefulness of any information, apparatus, product, or process disclosed, or represents that its use would not infringe privately owned rights. Reference herein to any specific commercial product, process, or service by trade name, trademark, manufacturer, or otherwise does not necessarily constitute or imply its endorsement, recommendation, or favoring by the United States government or Lawrence Livermore National Security, LLC. The views and opinions of authors expressed herein do not necessarily state or reflect those of the United States government or Lawrence Livermore National Security, LLC, and shall not be used for advertising or product endorsement purposes.

This work performed under the auspices of the U.S. Department of Energy by Lawrence Livermore National Laboratory under Contract DE-AC52-07NA27344.

Neutron inelastic scattering measurements on KCl and NaCl samples at the Dome

M.A. Stoyer, B. Longfellow, M. Burks, P.L. Kerr, and V.V. Mozin

Nuclear and Chemical Sciences Division, Lawrence Livermore National Laboratory, Livermore, CA 94550

E. Rubino

Weapons and Complex Integration Directorate, Lawrence Livermore National Laboratory, Livermore, CA 94550

Precise and accurate measurements of neutron inelastic scattering cross sections are vital for both the LLNL national security mission and for scientific applications such as the nuclear spectroscopy of planetary bodies. In this work, initial measurements of relative cross sections were performed by irradiating KCl and NaCl samples with a DD neutron generator, a DT neutron generator, and a PuB source in building 262, the Dome. The measurements allowed the existing experimental setup to be benchmarked. Several improvements to the setup are suggested for future experiments.

INTRODUCTION

Knowledge of the neutron inelastic scattering ($n, n'\gamma$) cross sections on a variety of elements is important for the WCI and SSP verification and validation efforts. In addition, these neutron-induced cross sections are vital inputs for measurements of the composition of planetary bodies via γ -ray spectroscopy both passively from cosmic ray spallation and actively from neutron generators delivered on spacecraft⁰. Recent work with a focus on the planetary nuclear spectroscopy application has suggested significant discrepancies between measured neutron inelastic scattering cross sections and the existing cross section libraries⁰. Consequently, our team was challenged to make some measurements and develop a method for improving the quality of the known data using 14 MeV neutrons and to extend the measurements to other neutron energies. We chose to concentrate our initial efforts on samples of KCl and NaCl, as the recent measurements of the ^{35}Cl and ^{37}Cl cross sections by P. N. Peplowski, *et al.* seemed to compare favorably with several nuclear data evaluations¹. The two samples chosen would provide several interesting tests—namely the determination of $^{35,37}\text{Cl}$ from different chemical matrices, a comparison with the ^{23}Na cross section that has been measured previously, and a possible initial measurement of ^{39}K and ^{41}K cross sections.

We chose to utilize an existing experimental setup at LLNL in the Dome, to enable rapid startup and provide some additional comparisons with other measurements that had been made previously on materials such as stainless steel and rock samples to support planetary spectroscopy missions. In these previous measurements, large samples were required (on the order of several kg of target material) so that sufficient statistics could be collected with irradiation times of roughly three hours. Therefore, for our work, we would also be able to take advantage of the presence of the naturally occurring radioactive ^{40}K in the large KCl sample to determine the effects of sample geometry and mass on our measurements.

Simplified level schemes for the various isotopes in the KCl and NaCl samples are shown in Figs. 1, 2, and 3 indicating the low-lying gamma-rays likely to be observed in these experiments².

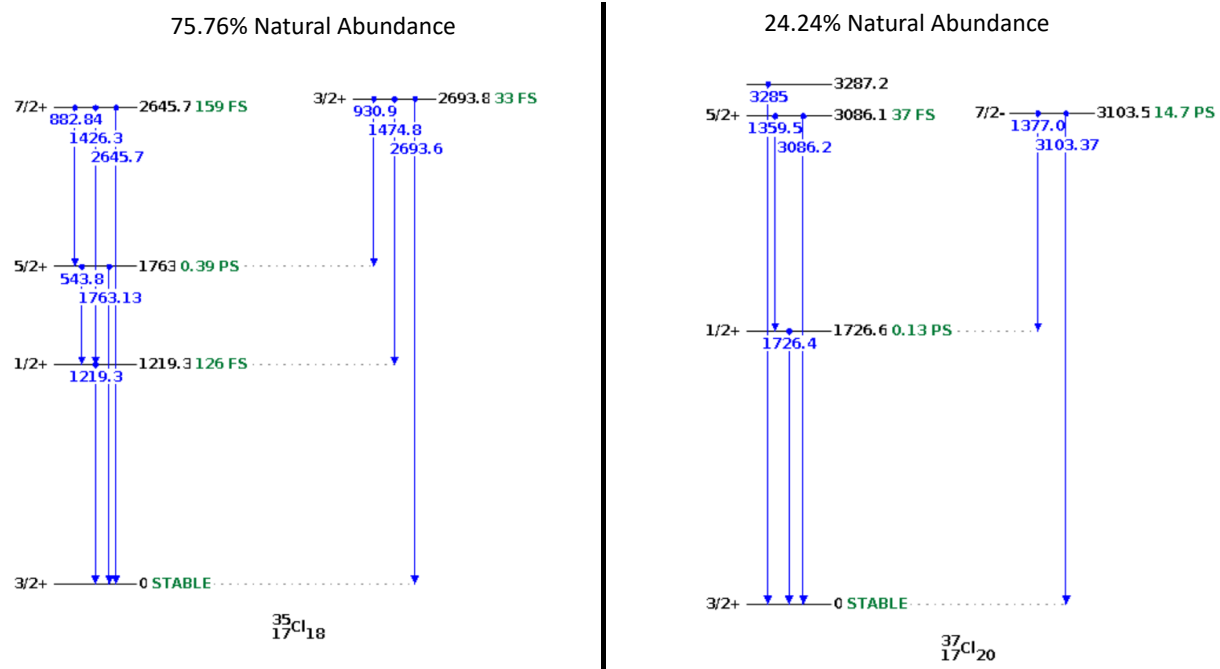


Fig. 1: The simplified low-lying level schemes of ^{35}Cl and ^{37}Cl from the National Nuclear Data Center (NNDC) database². Gamma-rays with energies of 1762(3) and 1218(9) keV and 1725(6) keV were observed from inelastic neutron scattering.

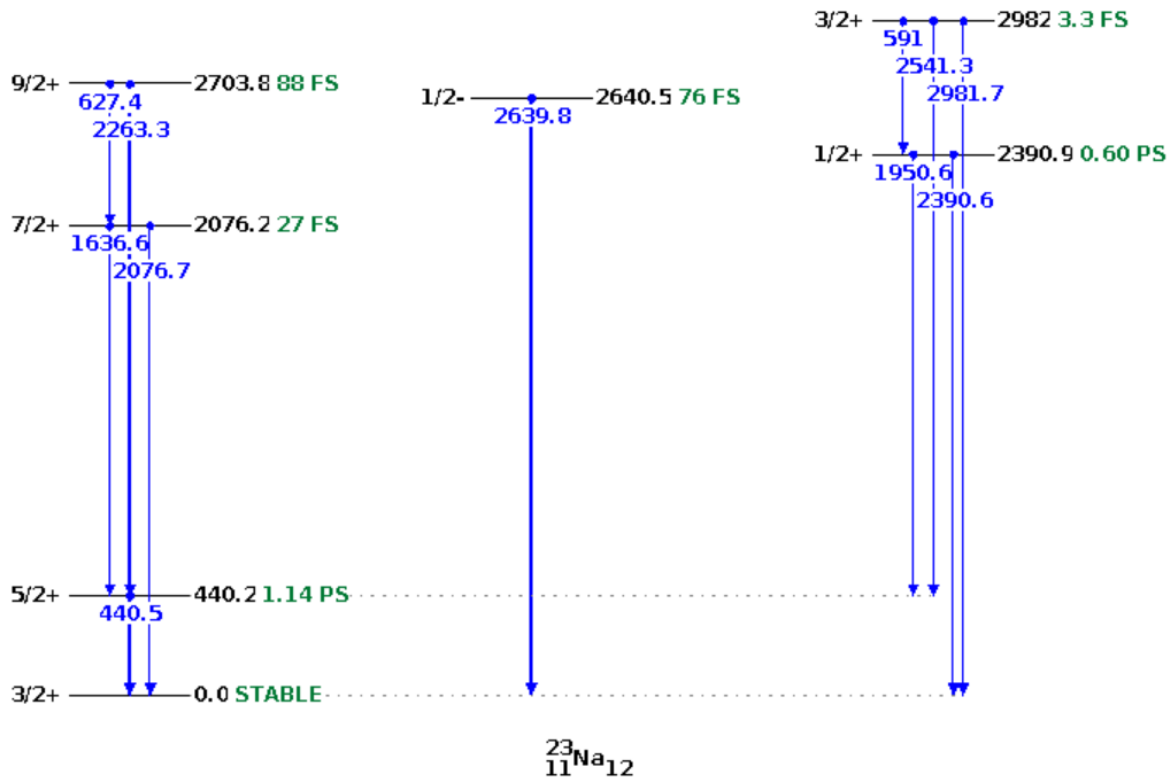


Fig. 2: Simplified low-lying level scheme for ^{23}Na from the National Nuclear Data Center (NNDC) database². The 440-keV gamma-ray was observed, and others expected from inelastic neutron scattering.

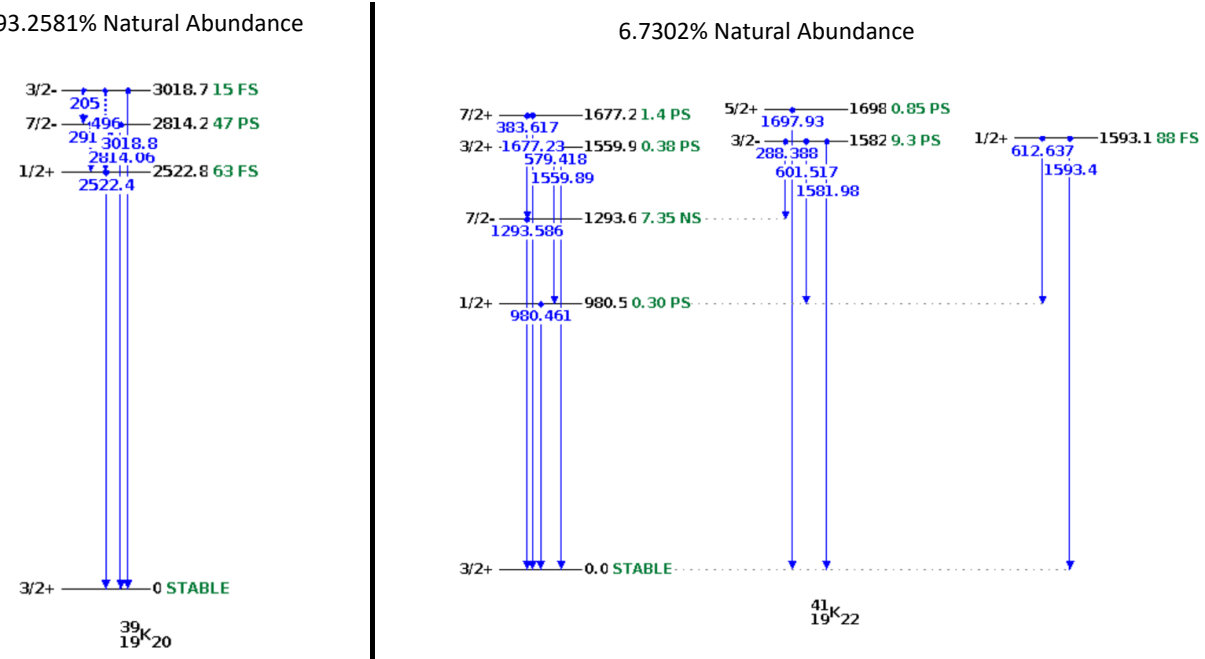


Fig. 3: Simplified low-lying level schemes for ^{39}K and ^{41}K from the National Nuclear Data Center (NNDC) indicating the likely gamma-rays from inelastic neutron scattering². The 2812(4)-keV and 1292(3)-keV gamma-rays from ^{39}K and ^{41}K , respectively, were observed in these experiments.

EXPERIMENTAL DETAILS

The experiment was run at LLNL in building 262, the Dome. The building is designed for neutron experiments having a concrete floor that is hollowed out underneath and high vaulted ceilings. The purpose of the experiment was to determine if the setup could be used for $(n, n'\gamma)$ measurements and if not, how to improve the setup.

The setup consisted of one high-purity germanium (HPGe) detector that was annealed prior to these experiments, one sample, one neutron source, and shielding. The HPGe detector was energy and efficiency calibrated using lines from ^{241}Am , ^{60}Co , ^{137}Cs , and ^{232}U sources. Additionally, background runs (without the samples) were collected both with and without the neutron sources on.

The experiment was configured with 2 different samples and 3 different neutron sources. The samples that were chosen have previously reported $(n, n'\gamma)$ data that was used as a benchmark, these are reagent grade sodium chloride (NaCl) and potassium chloride (KCl). The 2.5 kg of NaCl is contained in a 13 cm in diameter and 16 cm in height plastic container. The 2.5 kg KCl sample is contained in a 12.8 cm diameter and 21 cm height plastic container. The samples were placed on a few centimeters above the neutron sources with the HPGe at $\sim 90^\circ$ relative to the source containers.

The neutron sources consisted of a deuterium-tritium (DT) neutron generator, a deuterium-deuterium (DD) neutron generator, and plutonium-boron (PuB) source. The DT generator has a flux of $1.48 \times 10^7 \pm 15\%$ neutrons per second of 14 MeV neutrons and was operated at 20 μA and 60 kV. The DD generator has a flux of $1.3 \times 10^7 \pm 15\%$ neutrons per second of 2.5 MeV neutrons and was operated at 70 μA and 30 kV. The PuB source (decay corrected to the date used) has a flux of $4.70 \times 10^6 \pm 3\%$ neutrons per second with a range of energies to 5 MeV with the highest relative intensity at ~ 3 MeV, illustrated in Fig. 4.

The experiment details are given in Table 1 and consisted of both runs with the samples, and active background runs with no samples present. The experiments occurred between July 2022 and October 2022, with the long room background obtained in November 2022. Additionally, both samples were counted with no source of neutrons. The naturally occurring ^{40}K was used to determine a counting efficiency at 1460.8 keV for that extended sample in its position near the detector. Point sources located precisely at 30 cm from the HPGe were used to determine a relative efficiency curve as a function of gamma-ray energy.

Table 1: List of experimental details

| Run | Sample | Duration (s) | No. Neutrons emitted from source into 4π |
|-----------------|--------|--------------|--|
| Room background | None | 172612 | 0 |
| DT | KCl | 9296.5 | 1.38×10^{11} |
| DT | NaCl | 9360.6 | 1.39×10^{11} |
| DT | None | 9595.9 | 1.42×10^{11} |
| DD | KCl | 9424.7 | 1.23×10^{11} |
| DD | NaCl | 9574.8 | 1.24×10^{11} |
| DD | None | 9467.6 | 1.23×10^{11} |
| PuB | KCl | 205384 | 9.65×10^{11} |
| PuB | NaCl | 131073 | 6.16×10^{11} |
| PuB | None | 207846 | 9.77×10^{11} |

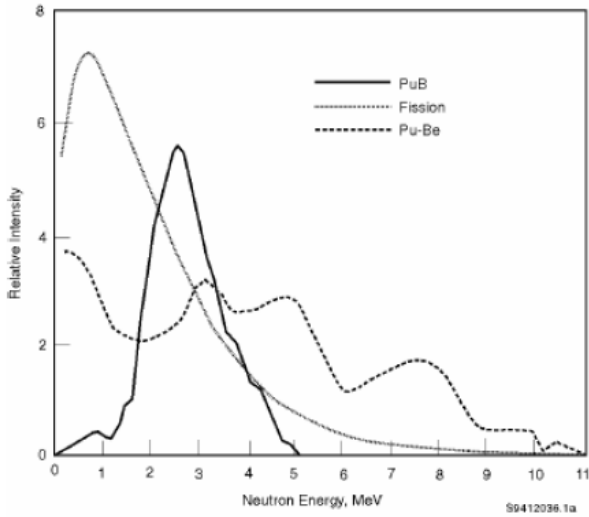


Fig. 4: The neutron energy in MeV vs. the relative intensities is shown. The PuB distribution of neutron energies is represented by the solid black curve³.

The shielding consisted of bismuth bricks to reduce the background neutrons interacting with the room as well as “collimate” the neutron beam reducing neutron scattering. Borated polyethylene was also used (white sheets with circular cutouts shown in Fig. 5) to reduce the neutron background.



Fig. 5: The experimental setup consists of (from left bottom to right top) borated polyethylene, a neutron source, a sample separator and the KCl sample, bismuth bricks, a collection of foam to prop the HPGe detector up, and finally the HPGe detector. The HPGe detector was about 10 cm from the edge of the samples.

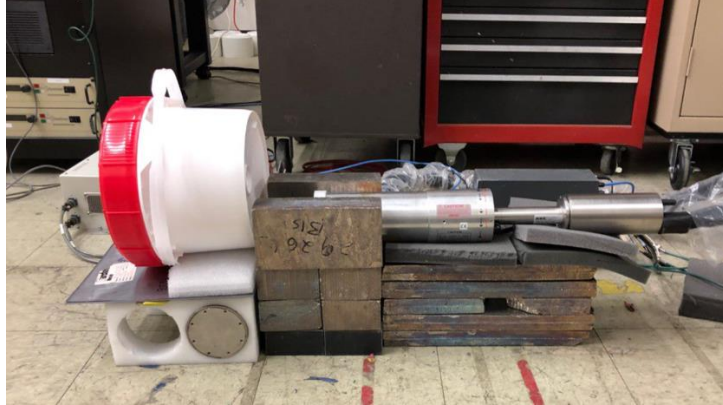


Fig. 6: Same as Fig. 5 except showing the NaCl sample.

RESULTS AND DISCUSSION

The efficiency curve for the HPGe detector constructed using well-calibrated point sources of ^{241}Am , ^{60}Co , ^{137}Cs and ^{232}U located at 30 cm from the front of the detector is shown in Figure 7. Note that this was significantly farther than the samples were placed for active neutron runs in order to reduce the deadtime of the detector. Efficiencies were measured for gamma-ray energies between 60 keV and 2.6 MeV and are shown in Figure 4 (blue circles). The amount of ^{40}K in the KCl sample was determined from the mass and its natural abundance to be $1.12 \mu\text{Ci}$, resulting in rate of 1460.8-keV gamma-rays of 4430 $\gamma/\text{s} \pm 1.5\%$. As this gamma-ray was emitted from throughout the volume of the KCl sample, it serves as our estimate of the geometrical effects of an extended distributed source. Self-attenuation was neglected. This value was used to scale the relative efficiency curve to approximately correct for the geometry of the sample and for the fact that the point sources and samples were located at different counting distances from the detector. This procedure results in the grey circles in Figure 7, and the fitted curve shown in the upper left of Fig. 7 was used to calculate gamma-ray rates for the various neutron irradiations. Note that the uncertainties in the scaled efficiencies are 4.2%; the propagated uncertainties of the various gamma-ray peak fits ($\sim 1\%$ or less), the source uncertainties ($\sim 3\%$) and the ^{40}K scaling factor uncertainty of 1.5%.

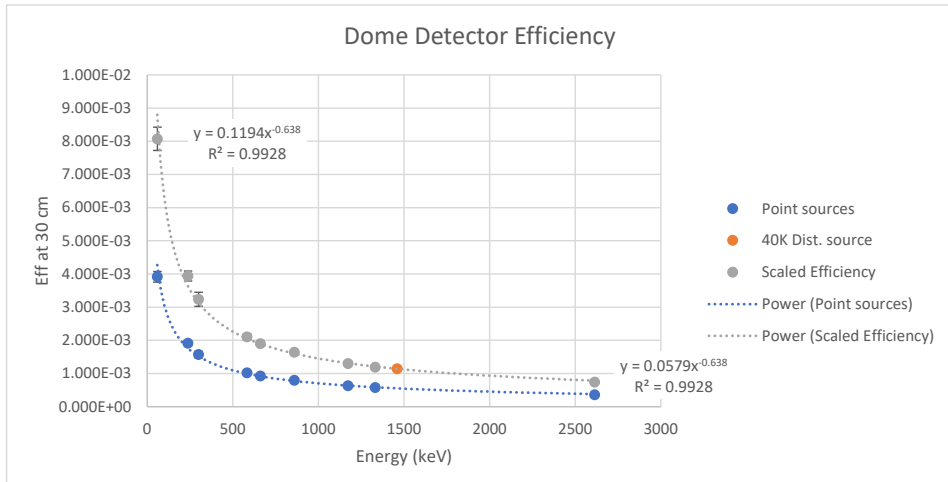


Fig. 7: Efficiency curve for the HPGe detector used in these experiments.

Spectra were obtained for all the runs detailed in Table 1. To correct for neutron source induced effects in the materials surrounding the experiment and other background, the spectra obtained with neutron sources active but with no sample present were subtracted from the spectra obtained with samples present, normalized by live-time. The resulting background subtracted spectra were then analyzed and the gamma-ray peaks fit using the FITEK peak fitting code developed at LLNL by Dr. Wolfgang Stoeffl. Because of neutron damage in the HPGe detector, the peaks were not pure Gaussians, but could be fit with reasonable quality by a Gaussian and low energy tail. The fit qualities ranged from χ^2/DF of 1 to 20 depending on the spectral region being analyzed. Better annealing of the detector and both the background subtraction and fitting could be improved to reduce uncertainties in future experiments. An example spectrum is shown in Figure 8.

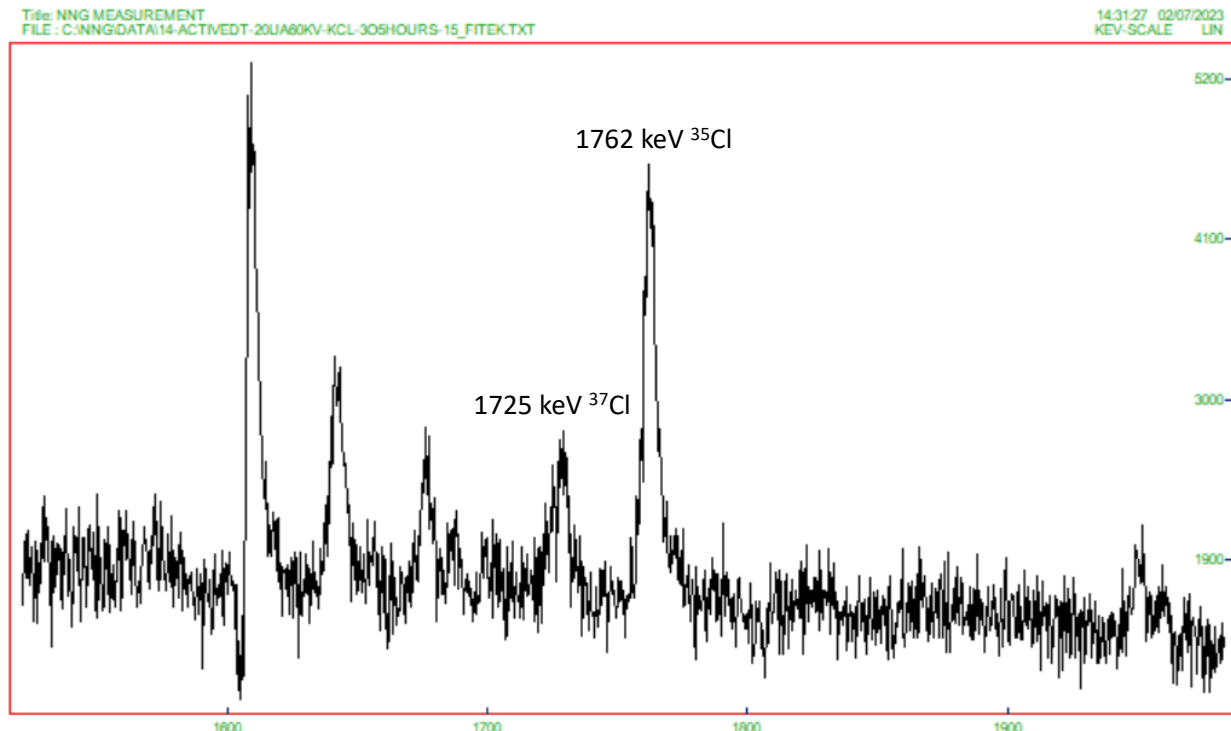


Fig. 8: Background subtracted gamma-ray spectrum from DT (14 MeV) neutron irradiation of a KCl sample. The ^{35}Cl and ^{37}Cl gamma-ray peaks are indicated.

Modeling of the experimental setup using Monte Carlo codes such as MCNP, GEANT, and MERCURY could be used to determine the numbers of neutrons actually impinging on the extended sample volumes. Simple models of the experimental setup were constructed, however, as seen in Fig. 5 and 6, the large and cumbersome shapes of the samples and the irregular shielding blocks are difficult to accurately model. Furthermore, the technical details of the of the HPGe detector such as the size of the germanium crystal were not available.

We report here gamma-ray intensity ratios for a variety of gamma-rays in ^{35}Cl , ^{37}Cl , ^{23}Na , ^{39}K and ^{41}K as shown in Table 2. The ratios are corrected for numbers of target atoms present in the sample (natural abundances), numbers of neutrons emitted from the various sources, varying count times, and scaled gamma-ray efficiencies. The ratios for DT generated neutrons (14 MeV) can be compared with prior measurements reported in an IAEA report⁴ and shown in Table 3.

Table 2: Gamma-ray emission ratios observed in these experiments normalized to the 1762-keV gamma-ray in ^{35}Cl .
The ratio uncertainties shown are statistical propagated errors.

| Isotope | Energy (keV) | DT+KCl | | DT+NaCl | | DD+KCl | | DD+NaCl | | PuB+KCl | | PuB+NaCl | |
|------------------|--------------|----------------|---------|----------------|---------|----------------|---------|----------------|---------|----------------|---------|----------------|---------|
| | | Ratio (X/1762) | Unc (%) |
| ^{35}Cl | 1762 | 1.00 | 8.8% | 1.00 | 8.3% | 1.00 | 8.7% | 1.00 | 9.3% | 1.00 | 7.6% | 1.00 | 6.8% |
| ^{35}Cl | 1218 | 0.70 | 9.1% | 0.38 | 10.5% | 0.82 | 9.4% | | | 1.03 | 8.1% | 1.27 | 7.6% |
| ^{37}Cl | 1725 | 1.00 | 12.3% | | | 0.65 | 14.3% | | | 0.84 | 8.0% | 0.80 | 7.1% |
| ^{39}K | 2812 | 1.11 | 8.6% | | | 0.02 | 34.1% | | | 0.16 | 7.7% | | |
| ^{41}K | 1292 | 1.94 | 25.0% | | | 0.70 | 26.7% | | | 3.07 | 9.3% | | |
| ^{23}Na | 440 | | | 3.20 | 7.4% | | | 4.64 | 9.7% | | | 3.45 | 6.5% |

Table 3: Gamma-ray emission ratios observed prior for a 14-MeV neutron source⁴.

| Isotope | Energy (keV) | 14 MeV IAEA Ratio | 14 MeV IAEA Unc (%) |
|------------------|--------------|-------------------|---------------------|
| ^{35}Cl | 1762 | 1.00 | 38.5% |
| ^{35}Cl | 1218 | 0.61 | 34.3% |
| ^{37}Cl | 1725 | 1.83 | 41.1% |
| ^{39}K | 2812 | 0.47 | 28.0% |
| ^{41}K | 1292 | | |
| ^{23}Na | 440 | 3.85 | 29.7% |

Table 4: Gamma-ray emission ratios in the literature for neutrons at approximately 2.5 MeV.

| Isotope | Energy (keV) | Ratio | Unc |
|------------------|--------------|-------------------|------|
| ^{35}Cl | 1762 | 1.00 ^a | ~15% |
| ^{35}Cl | 1218 | 0.95 ^a | ~15% |
| ^{37}Cl | 1725 | 0.70 ^a | ~15% |
| ^{41}K | 978 | 0.78 ^b | ~15% |
| ^{23}Na | 440 | 2.25 ^c | ~13% |

^a2.54 MeV neutrons from Ref 5, ^b2.63 MeV neutrons from Ref 6, ^c2.50 MeV neutrons from Ref 7

As seen in the comparison between Tables 2 and 3, the ratios for the 1218-keV line from ^{35}Cl relative to the 1762-keV line from ^{35}Cl in DT+KCl and DT+NaCl are relatively consistent with the IAEA value. However, the 1725-keV gamma ray from ^{37}Cl is absent in the DT+NaCl data despite being clearly observed in the KCl data of Figure 5. Furthermore, the present ratio for the 440-keV line from ^{23}Na is relatively consistent with the literature but the ratio for the 2812-keV line from ^{39}K is over a factor of two larger than the IAEA ratio. For the DD+KCl data, the 1218-keV and 1725-keV ratios from Cl agree well with the literature values in Table 4 but a line at 978 keV from ^{41}K observed previously⁵ was not seen here. The 1292 keV line observed in the present work from ^{41}K was not reported in Ref 5. Moreover, the 1218-keV and 1725-keV lines from Cl were not observed in the DD+NaCl data from this work.

It should be noted that there was a significant difference in overall count rate between the two samples and various combinations of neutron sources as shown in Table 5. The large numbers of peaks remaining in the PuB data even after background subtraction suggests the presence of more complicated gamma-ray backgrounds perhaps including fission product gamma-rays. In general, the DD source operated at lower count rates overall and had fewer numbers of potentially interfering peaks, and may provide a simpler case for modelling of the results and validation efforts.

The 1725-keV gamma-ray peak from ^{37}Cl in the NaCl sample was obscured in several spectra by the presence of a large background blob which when subtracted could have over-subtracted any actual small peak (see Figures 9 and 10). These different background profiles between the KCl and NaCl samples may explain why the 1725-keV gamma ray from ^{37}Cl was not observed in the DT+NaCl and DD+NaCl runs.

The estimated uncertainties from this work are the statistical errors only, but these uncertainties are already in many cases significantly less than the uncertainties in the IAEA report⁴ and shown in Table 3. This indicates that the method may produce higher quality data than currently exists with the improvements discussed in the Conclusions section. However, it should be noted that for cross section measurements using the ratio method, the uncertainty on the standard has to be taken into account. Consequently, the overall uncertainty on the measured cross section cannot be smaller than the uncertainty on the standard.

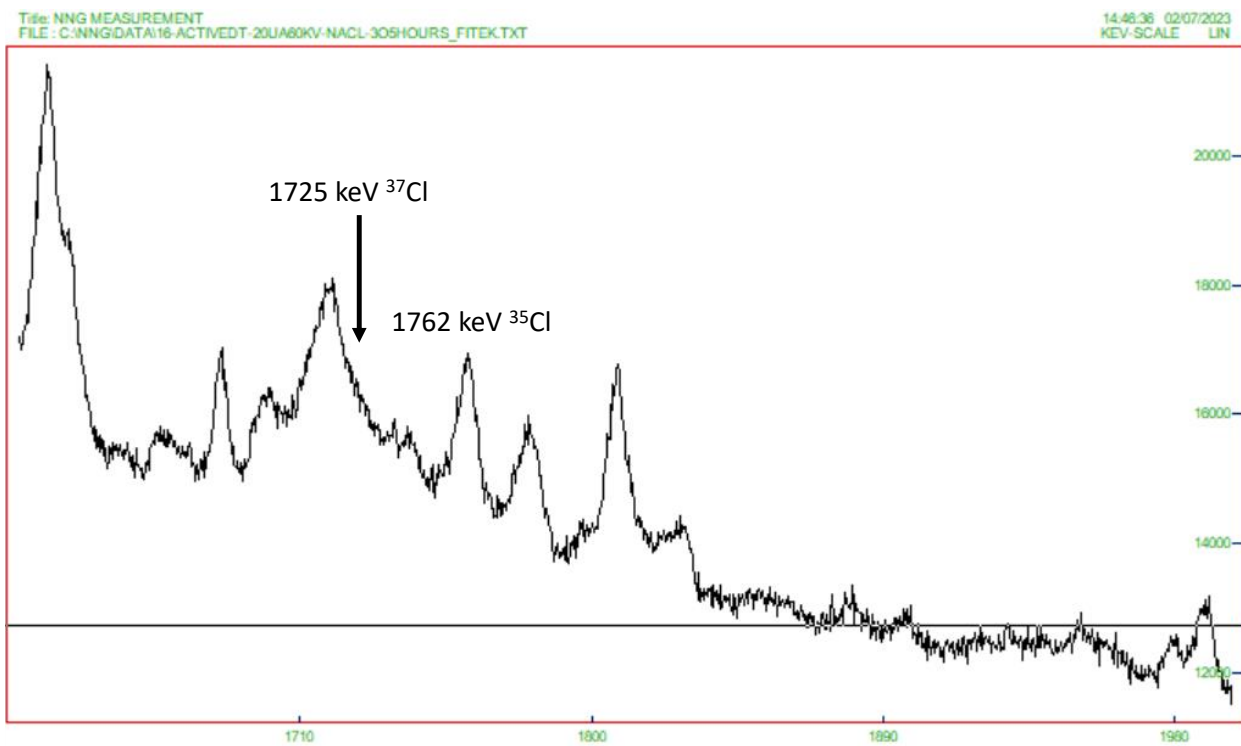


Fig. 9: Un-background subtracted gamma-ray spectrum from DT (14 MeV) neutrons on NaCl sample showing the background in the region of the ^{35}Cl and ^{37}Cl peaks.

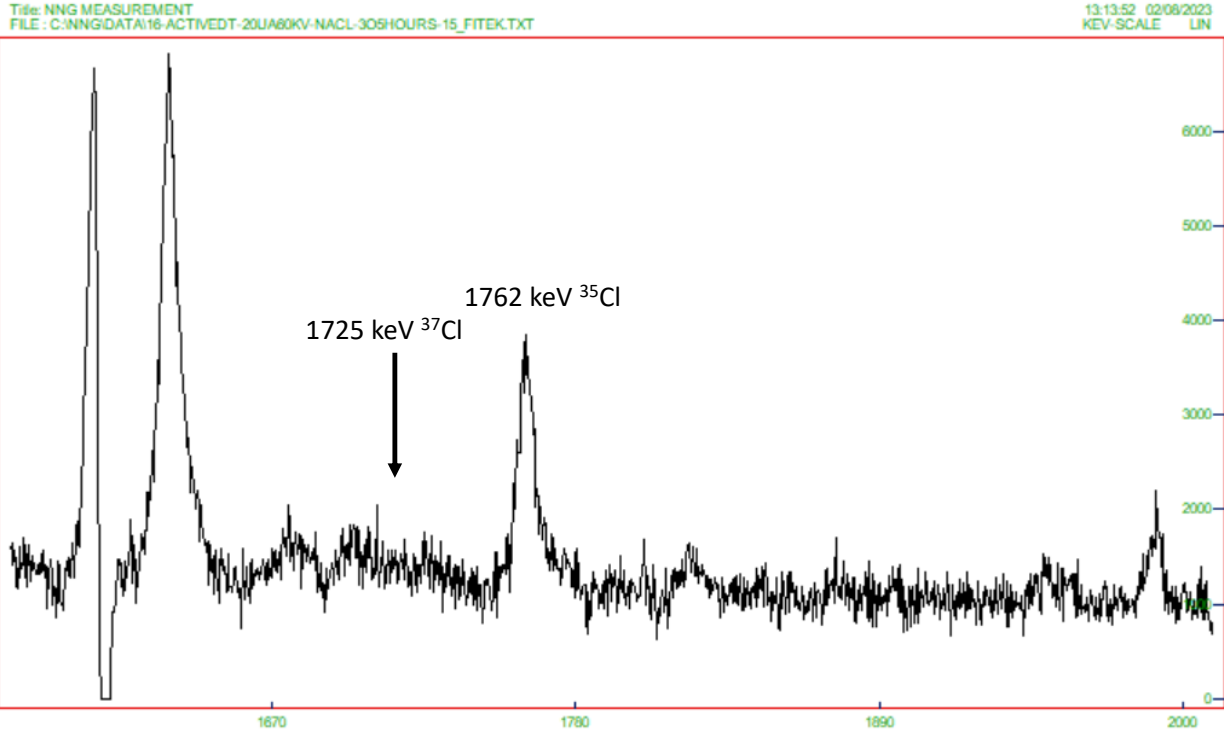


Fig. 10: Background subtracted gamma-ray spectrum from DT (14 MeV) neutrons on NaCl sample showing the background in the region of the ^{35}Cl and ^{37}Cl peaks and lack of 1725-keV peak.

Table 4: Comparison of overall detector counting rate and numbers of observed gamma-ray peaks in the spectra for the two different samples and three different neutron sources. For future work, depending on the isotopes being measured and the complexity of the nuclear level schemes, one might consider using a given neutron source over another in order to reduce potential gamma-ray peak interferences and background.

| Measurement | KCl Sample | | NaCl Sample | |
|-------------|-----------------------------------|---|-----------------------------------|---|
| | Overall detector count rate (cps) | Rough number of gamma peaks in spectrum | Overall detector count rate (cps) | Rough number of gamma peaks in spectrum |
| Background | 229 | 18 | 143 | 21 |
| DD | 1530 | 17 | 606 | 7 |
| DT | 5007 | 30 | 4109 | 16 |
| PuB | 1867 | 79 | 2575 | 65 |

CONCLUSIONS AND FUTURE WORK

While the present experimental efforts in the dome were able to yield some cross section ratios that were reasonably consistent with values in the literature, other ratios were inconsistent with known data. In addition, the 1725-keV ^{37}Cl gamma ray was clearly observed from the KCl sample but was not observed from the NaCl sample using the DD and DT generators. This lack of consistency makes the current setup difficult to trust for tests of the existing nuclear data libraries. However, several improvements to the setup can be made to allow for the extraction of precise and accurate nuclear data. Neutron inelastic

scattering cross section measurements rely on both a well-characterized gamma-ray detection efficiency and a well-characterized neutron flux.

The gamma-ray detection efficiency can be better constrained by using samples with a standardized geometry for irradiation. In addition, the use of smaller samples placed further away from the gamma-ray detector would more closely match the conditions of standard calibration sources allowing a more accurate determination of the energy-dependent detection efficiency. At the same time, this would make simulating the experimental setup easier and reduce detector deadtime but would require longer counting times. To compensate, additional high-purity germanium detectors could be added which would enable the measurement of angular distributions. BGO Compton suppression shielding can be added to the germanium detectors to improve the peak-to-total of the setup. Furthermore, borated polyethylene shielding can be employed to reduce background from neutron-induced reactions.

The neutron flux from the DD and DT generators could be better characterized by using the multi-foil activation method. Again, moving the generators further away from the samples would reduce geometrical effects making the number of neutrons impinging on the sample easier to calculate or model. To reduce neutron scattering, collimation could be employed to produce a more beam-like profile of neutrons. However, this may require the use of a higher flux neutron generator. Alternatively, for the DT generator, absolute measurements of the neutron flux during runs can be made with an Associated Particle Imaging (API) system. The API would provide the additional opportunity to tag on alpha-gamma coincidences to reduce time-random background.

ACKNOWLEDGEMENTS

This work was performed under the auspices of the U.S. Department of Energy by Lawrence Livermore National Laboratory under contract DE-AC52-07NA27344. The authors would like to profusely thank Drs. Vladimir Mozin and Phil Kerr for the high-quality collection of the experimental data and performance of the many experimental runs in the Dome.

REFERENCES

⁰See for example—<https://dragonfly.jhuapl.edu/>

¹Patrick N. Peplowski, Jack T. Wilson, Mauricio Ayllon-Unzueta, Workshop for Applied Nuclear Data Activities (WANDA) 2 March 2022, slide 11.

²<https://www.nndc.bnl.gov/>

³US DOE, DOE-STD-1128-98

⁴S.P. Simakov, A. Pavlik, H. Vonach, and S. Hlaváč, INDC(CCP)-413, IAEA final report, “*Status of Experimental and Evaluated Discrete Gamma-ray Production at $E_n=14.5\text{ MeV}$* ”, (1998).

⁵D. B. Nichols, B. D. Kern, and M. T. McEllistrem, Phys. Rev. 151, 879 (1966).

⁶D. B. Nichols and M. T. McEllistrem, Phys. Rev. 166, 1074 (1967).

⁷J. R. Vanhoy *et al.*, Nucl. Phys. A 939, 121 (2015).